

**Electronic Supplementary Information**

**Tantalum(IV) pyrazolate: new wine in the old wineskin**

Pavel A. Petrov,<sup>\*a</sup> Yuliya A. Laricheva,<sup>a</sup> Taisiya S. Sukhikh<sup>a</sup> and Maxim N. Sokolov<sup>a</sup>

<sup>a</sup> Nikolaev Institute of Inorganic Chemistry, Siberian Branch of Russian Academy of Sciences,

Novosibirsk, Russia

Fax: +7 (383) 316 9489;

Tel: +7 (383) 316 5845;

E-mail: panah@niic.nsc.ru

## Experimental Section

### General remarks

All operations were carried out in evacuated Schlenk tubes using standard vacuum-line techniques (residual pressure  $<10^{-2}$  torr). All glassware was oven-dried at 125 °C overnight. Starting materials Ta(NMe<sub>2</sub>)<sub>5</sub> (Dalchem) and Hpz (Aldrich or TCI) were used as received from suppliers. Solvents were distilled in an inert atmosphere over common drying agents (THF – K/benzophenone, toluene – Na/benzophenone, C<sub>6</sub>D<sub>6</sub> – Na-K alloy), stored over Na-K alloy prior to use, and transferred under vacuum. <sup>1</sup>H NMR spectra (500.13 MHz) and <sup>13</sup>C NMR spectra (125.76 MHz) were taken with a Bruker DRX-500 spectrometer (Bruker Corporation, Billerica, MA, USA) in fire-sealed NMR tubes at ambient temperature; the solvent peak was used as the internal reference. The IR spectra were recorded in KBr pellets (prepared in argon-filled glove box) at room temperature by means of a FT-801 Fourier spectrometer (Simex, Novosibirsk, Russia). Elemental analysis was performed with a Eurovector EuroEA3000 analyzer (Eurovector SPA, Redavalle, Italy).

### Synthesis of [Ta<sub>2</sub>(pz)<sub>8</sub>] (1)

In a glovebox, Ta(NMe<sub>2</sub>)<sub>5</sub> (491 mg, 1.22 mmol) and pyrazole (423 mg, 6.21 mmol) were placed into a Schlenk tube equipped with J. Young PTFE valve. The tube was evacuated and cooled down to –196 °C, and *ca.* 20 mL of toluene was vacuum-transferred. After spontaneous heating to room temperature, a clear yellow solution was heated at 60 °C for 5 days causing gradual darkening. Resulting brown solution was evaporated *in vacuo*, and *ca.* 20 mL toluene was vacuum-transferred to the dark oily residue. The solution was transferred to L-shaped glass tube, which was then frozen down to –196 °C, evacuated to *ca.*  $<10^{-2}$  torr and fire-sealed. Slow evaporation of the solvent into on knee afforded almost black crystals of **1** suitable for X-ray analysis (549 mg, 50 %). <sup>1</sup>H NMR (C<sub>6</sub>D<sub>6</sub>): δ 5.46 (br s, 1H, CH<sup>4</sup> (bridging pz)), 5.73 (t, *J* = 2.1 Hz, 1H, CH<sup>4</sup> (terminal pz)), 6.31 (br s, 1H, CH<sup>3,5</sup> (bridging pz)), 7.38 (br s, 2H, CH<sup>3,5</sup> (terminal pz)), 8.09 (br s, 1H, CH<sup>3,5</sup> (bridging pz)). <sup>13</sup>C{<sup>1</sup>H} NMR (C<sub>6</sub>D<sub>6</sub>): δ 104.6, 111.2, 129.4, 137.7, 140.8. IR (KBr, cm<sup>-1</sup>): 3124 w, 3053 w, 2976 w, 2919 w, 1604 w, 1525 w, 1489 m, 1468 s, 1419 m, 1407 m, 1376 s, 1361 m, 1301 s, 1184 m, 1164 m, 1090 m, 1062 vs, 1007 m, 973 m, 921 m, 869 m, 757 vs, 611 s. Found: C, 31.85; H, 2.80; N, 25.00. Calc. for C<sub>24</sub>H<sub>24</sub>N<sub>16</sub>Ta<sub>2</sub>: C, 32.08; H, 2.69; N, 24.94%.

### NMR monitoring of the reaction of Ta(NMe<sub>2</sub>)<sub>5</sub> and pyrazole

In a glovebox, Ta(NMe<sub>2</sub>)<sub>5</sub> (10 mg, 0.025 mmol), pyrazole (8.5 mg, 0.125 mmol) and C<sub>6</sub>D<sub>6</sub> (0.6 mL) were placed into a 5 mm NMR tube. The tube cooled down to *ca.* –70 °C, evacuated and fire-sealed. <sup>1</sup>H NMR spectra were recorded after spontaneous heating to room temperature and then after heating at 60 °C for 24, 72 and 168 hours (see Fig. S4, S5).

### ESR monitoring of the reaction of Ta(NMe<sub>2</sub>)<sub>5</sub> and pyrazole

In a glovebox, Ta(NMe<sub>2</sub>)<sub>5</sub> (8 mg, 0.020 mmol), pyrazole (8 mg, 0.117 mmol) and THF (*ca.* 1 mL) were placed into a lambda-shaped two-side pyrex tube. The tube cooled down to *ca.* –70 °C, evacuated and fire-sealed. ESR spectra were recorded after spontaneous heating to room temperature and then after heating at 60 °C for 4 and 16 hours; no paramagnetic species were detected.

### DFT Calculations

Geometry optimizations, electronic structure analysis and topological analysis were carried out using Density Functional Theory (DFT) calculations from the ADF2019 program [1, 2]. The calculations were performed with standard Slater-type orbitals all-electron TZ2P+ basis set [3]. Relativistic corrections were introduced with the zeroth-order regular approximation (ZORA) [4]. As with the geometry optimization, the VWN (Local Density Approximation) [5] and Becke-Perdew (Generalized Gradient Approximation) [6, 7] functionals were used, spin-unrestricted, no imaginary frequencies were found. AIM calculation results were Poincare-Hopf satisfied.

## X-ray Structure Determination

Single-crystal XRD data for **1** were collected at 150 K with a Bruker Apex DUO diffractometer (Bruker Corporation, Billerica, MA, USA) equipped with a 4K CCD area detector and a graphite-monochromated sealed tube (Mo K $\alpha$  radiation,  $\lambda = 0.71073$  Å). The  $\phi$ - and  $\omega$ -scan techniques were employed to measure intensities. Absorption correction was applied with the use of the SADABS program [8]. The crystal structure was solved using the SHELXS [9] and was refined using SHELXL [10] programs with OLEX2 GUI [11]. Atomic thermal parameters for non-hydrogen atoms were refined anisotropically. The positions of hydrogen atoms were calculated corresponding to their geometrical conditions and refined using the riding model. The crystallographic data and structure solution details are given in Table S1. CCDC 2048282 contains the supplementary crystallographic data for this paper. These data can be obtained free of charge from the Cambridge Crystallographic Data Centre via [www.ccdc.cam.ac.uk/data\\_request/cif](http://www.ccdc.cam.ac.uk/data_request/cif) [12].

**Table S1.** Crystal data and structure refinement parameters of **1**.

Empirical formula	C <sub>24</sub> H <sub>24</sub> N <sub>16</sub> Ta <sub>2</sub>
Formula weight	898.49
Temperature, K	150(2)
Crystal system	monoclinic
Space group	<i>P</i> 2 <sub>1</sub> / <i>n</i>
<i>a</i> , Å	8.4335(17)
<i>b</i> , Å	14.985(3)
<i>c</i> , Å	22.574(5)
$\alpha$ , °	90
$\beta$ , °	96.76(3)
$\gamma$ , °	90
Volume, Å <sup>3</sup>	2833.0(10)
<i>Z</i>	4
$\rho_{\text{calc}}$ , g/cm <sup>3</sup>	2.107
$\mu$ , mm <sup>-1</sup>	7.766
<i>F</i> (000)	1704.0
Crystal size/mm	0.2 × 0.12 × 0.1
Radiation	MoK $\alpha$ ( $\lambda = 0.71073$ )
2 $\Theta$ range for data collection, °	4.538 to 57.394
Index ranges	$-8 \leq h \leq 11$ , $-20 \leq k \leq 17$ , $-30 \leq l \leq 30$
Reflections collected	22936
Independent reflections	7278 [ $R_{\text{int}} = 0.0357$ , $R_{\text{sigma}} = 0.0337$ ]
Data/restraints/parameters	7278/0/379
Goodness-of-fit on $F^2$	1.074
Final <i>R</i> indexes [ $I \geq 2\sigma(I)$ ]	$R_1 = 0.0232$ , $wR_2 = 0.0525$
Final <i>R</i> indexes [all data]	$R_1 = 0.0276$ , $wR_2 = 0.0542$
Largest diff. peak/hole, e Å <sup>-3</sup>	1.70/−1.21

**Table S2.** Selected bond lengths (Å) in single crystal XRD and DFT-optimized structures.

<b>Bond</b>	<b>XRD</b>	<b>DFT</b>	
		<b><i>S</i> = 0</b>	<b><i>S</i> = 1</b>
Ta1–Ta2	3.1895(7)	3.1450	3.6010
Ta1–N11	2.183(3)	2.1821	2.1689
Ta1–N12	2.189(3)	2.1834	2.1732
Ta1–N21	2.192(3)	2.1855	2.1696
Ta1–N22	2.159(3)	2.1827	2.1725
Ta2–N31	2.169(3)	2.1842	2.1719
Ta2–N32	2.172(3)	2.1852	2.1715
Ta2–N41	2.179(3)	2.1833	2.1714
Ta2–N42	2.189(3)	2.1844	2.1711
av. Ta–N (terminal)	2.18[1]	2.1839	2.1713
Ta1–N51	2.248(3)	2.2505	2.2841
Ta2–N52	2.130(3)	2.1266	2.1374
Ta1–N61	2.126(3)	2.1274	2.1376
Ta2–N62	2.258(3)	2.2508	2.2856
Ta1–N71	2.258(3)	2.2507	2.2845
Ta2–N72	2.128(3)	2.1283	2.1378
Ta1–N81	2.122(3)	2.1280	2.1379
Ta2–N82	2.248(3)	2.2490	2.2839
av. Ta–N (bridging)	2.19[7]	2.1885	2.2111

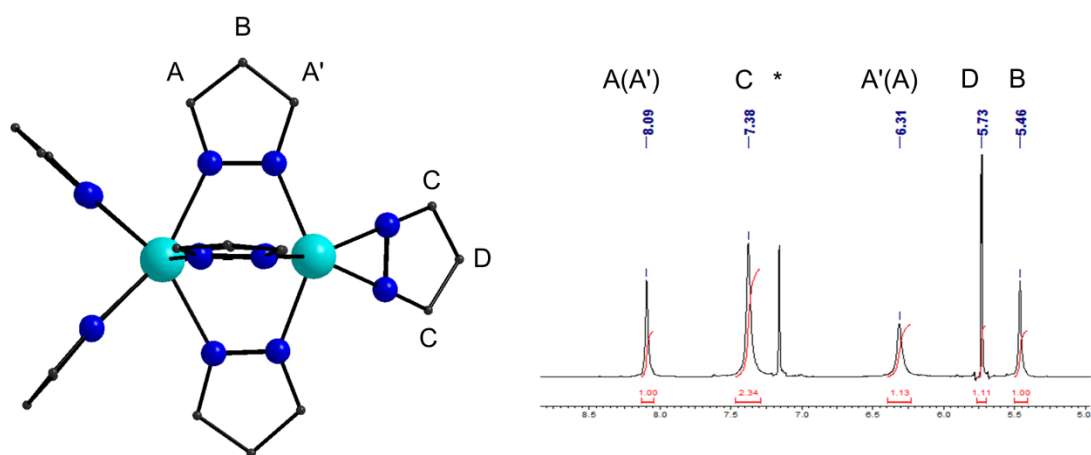
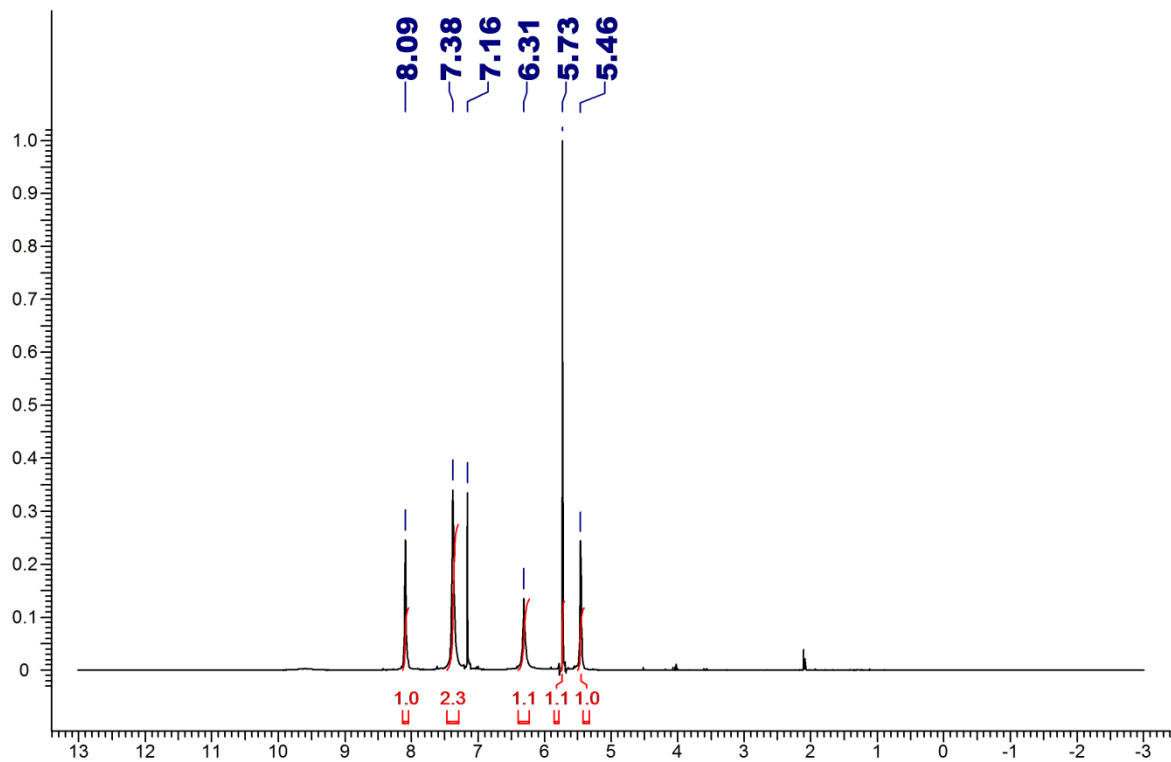


**Figure S1.** (top)  $^1\text{H}$  NMR spectrum of **1** ( $\text{C}_6\text{D}_6$ , 298K); (bottom) Attribution scheme. Asterisk denotes a residual benzene signal ( $\delta$  7.16).

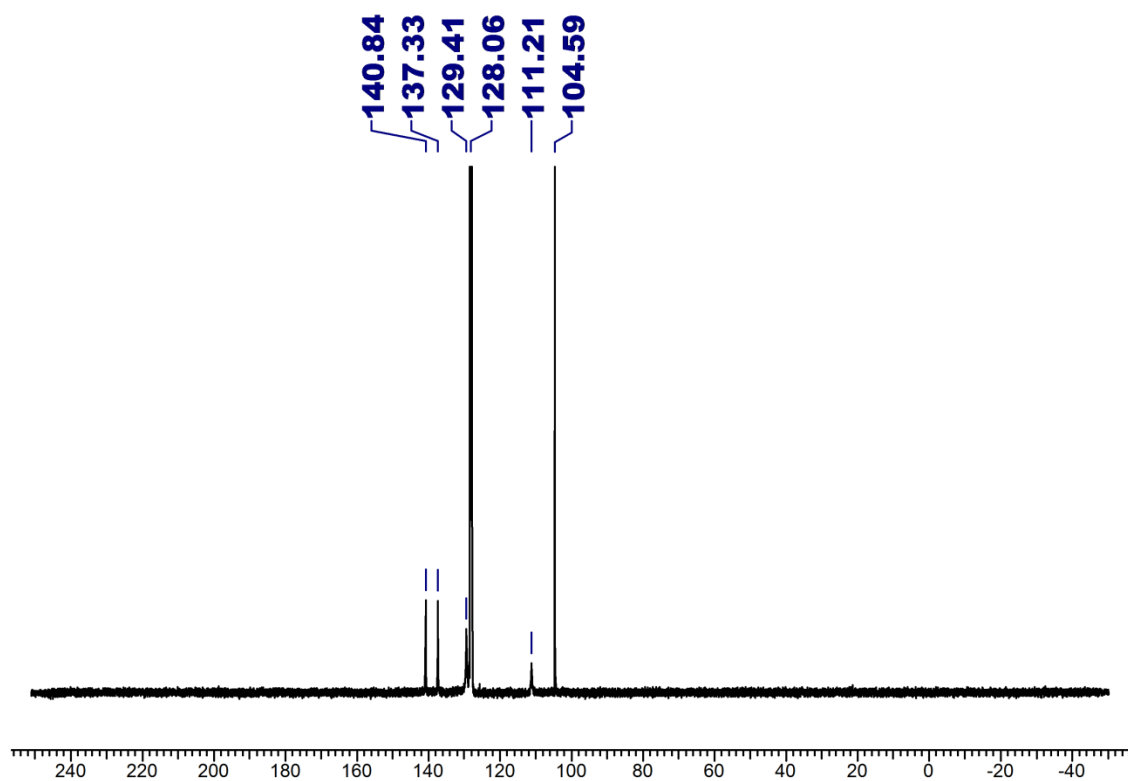


**Figure S2.**  $^{13}\text{C}$  NMR spectrum of **1** ( $\text{C}_6\text{D}_6$ , 298K).

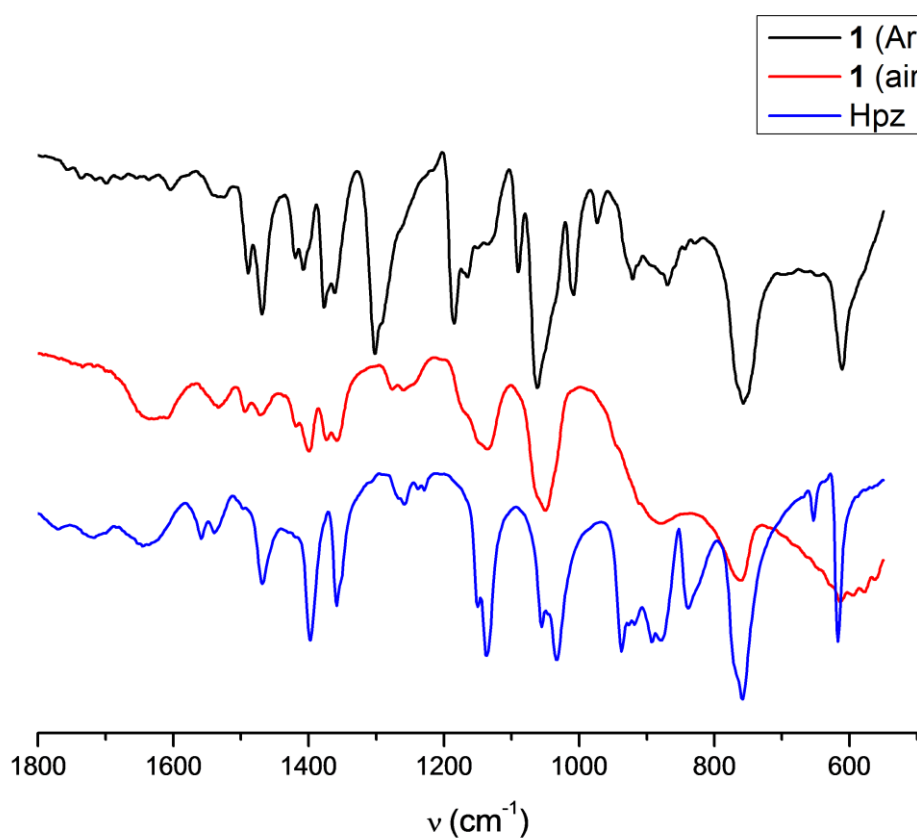
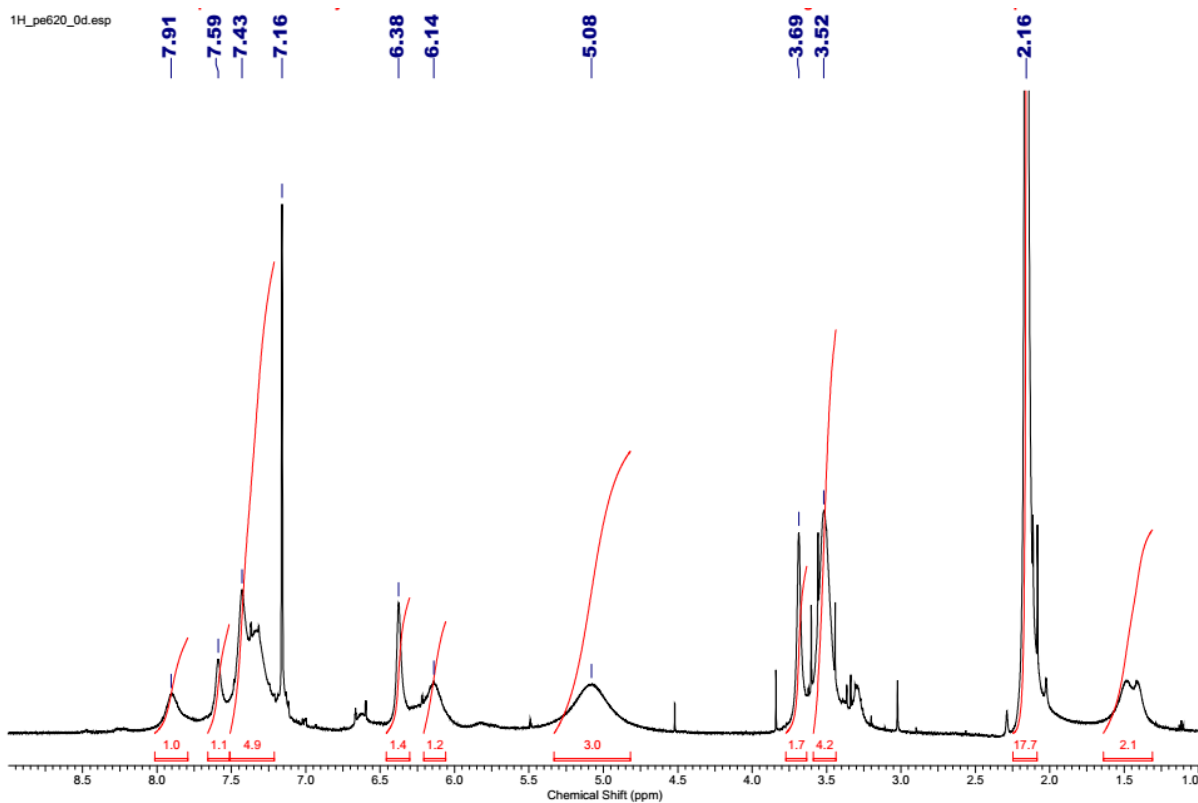
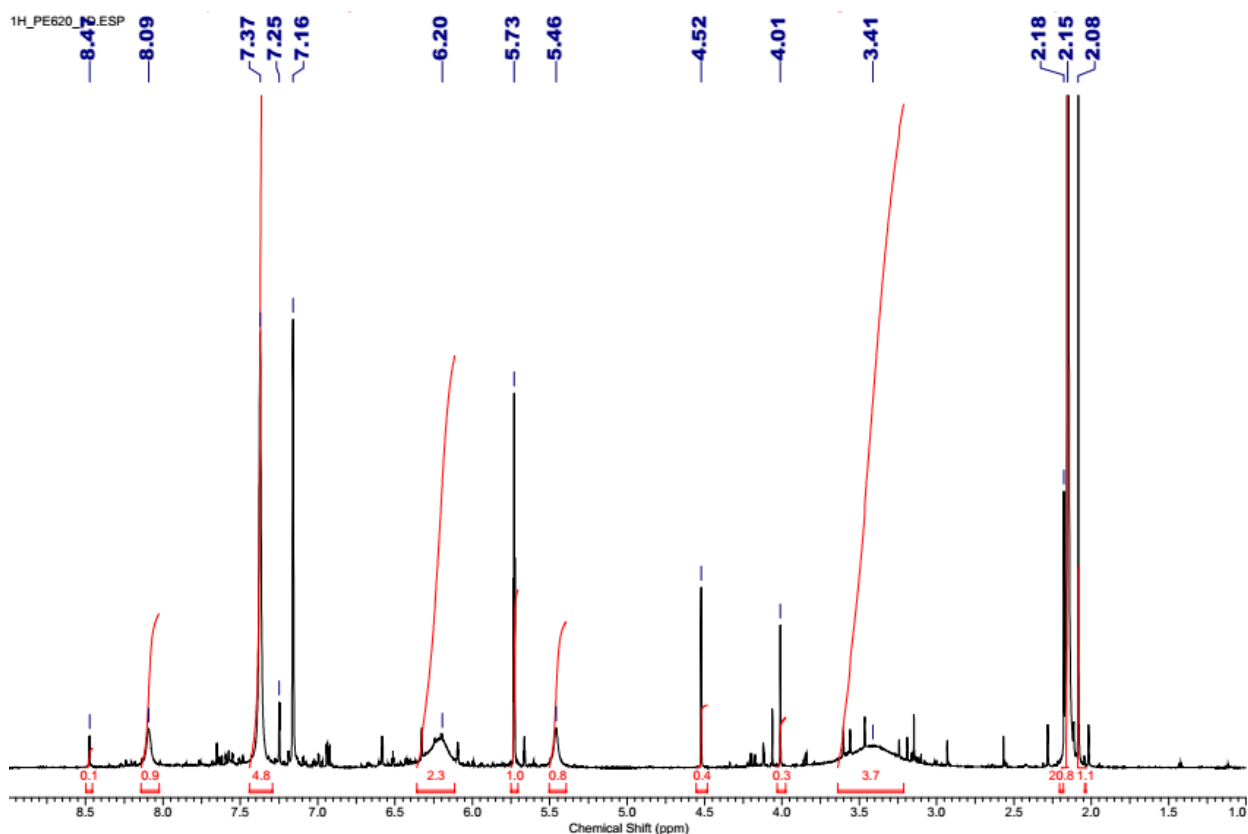


**Figure S3.** IR spectra in KBr: **1** in argon atmosphere (black); **1** after exposure to air (red); pyrazole (blue).

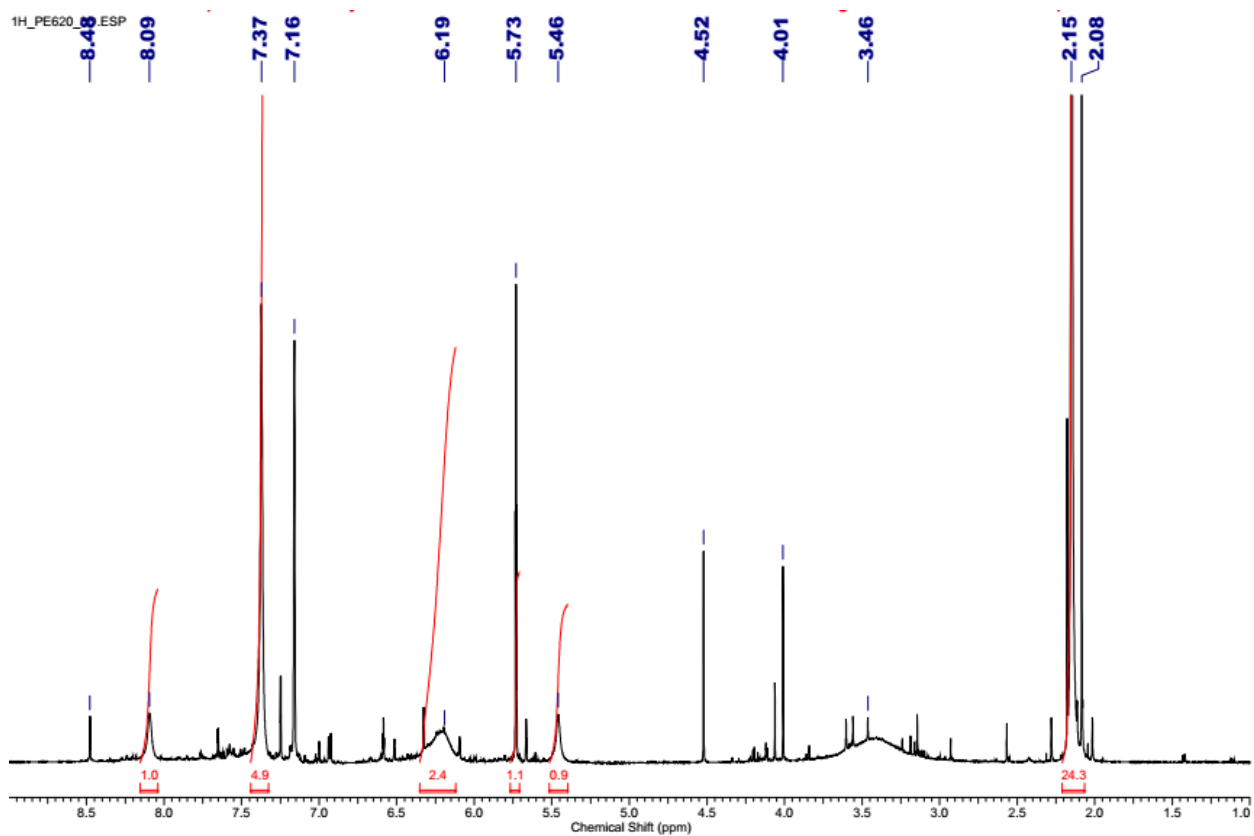


(a)

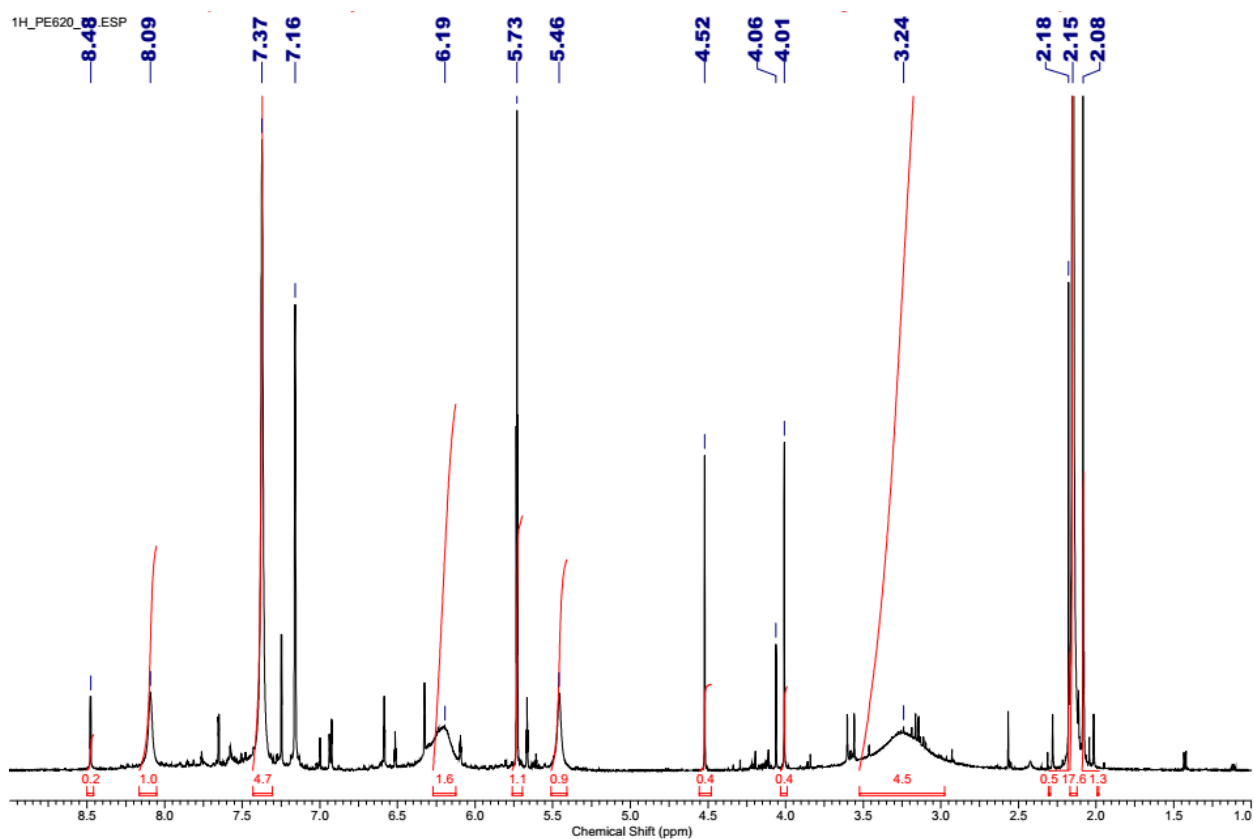


(b)

**Figure S4.**  $^1\text{H}$  NMR spectra of the reaction mixture ( $\text{Ta}(\text{NMe}_2)_5$ , 1 eq; Hpz, 5 eq;  $\text{C}_6\text{D}_6$ ) after mixing (a) and after heating for 24 h (b).



(a)



(b)

**Figure S5.**  $^1\text{H}$  NMR spectra of the reaction mixture ( $\text{Ta}(\text{NMe}_2)_5$ , 1 eq; Hpz, 5 eq;  $\text{C}_6\text{D}_6$ ) after heating for 72 h (a) and 168 h (b).



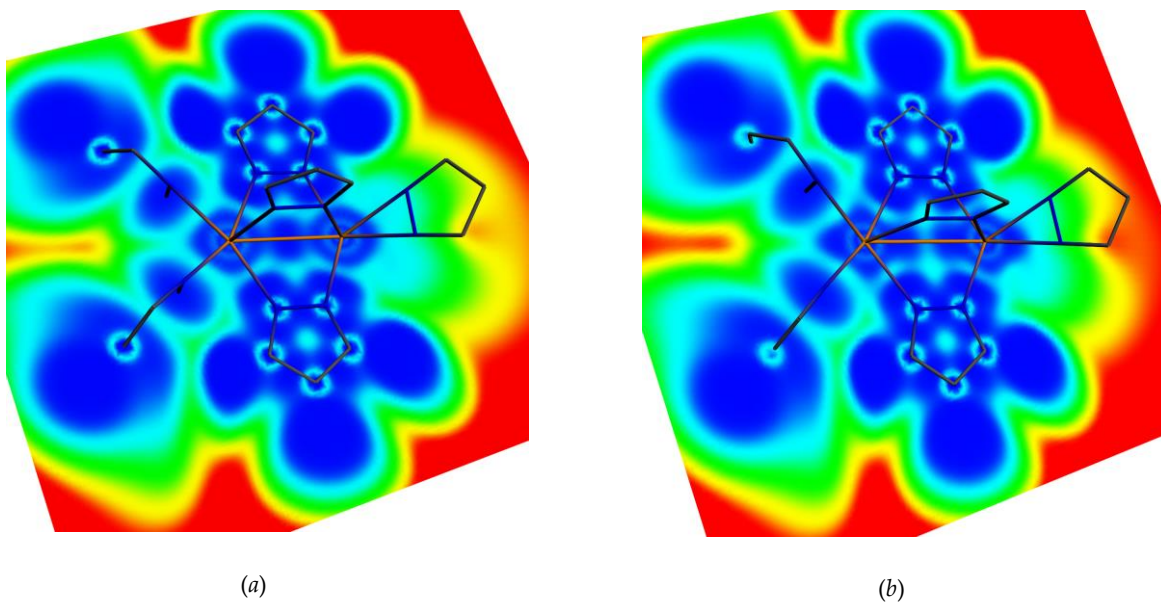


**Figure S6.** ELF cut planes: (a) Singlet spin state; (b) Triplet spin state.

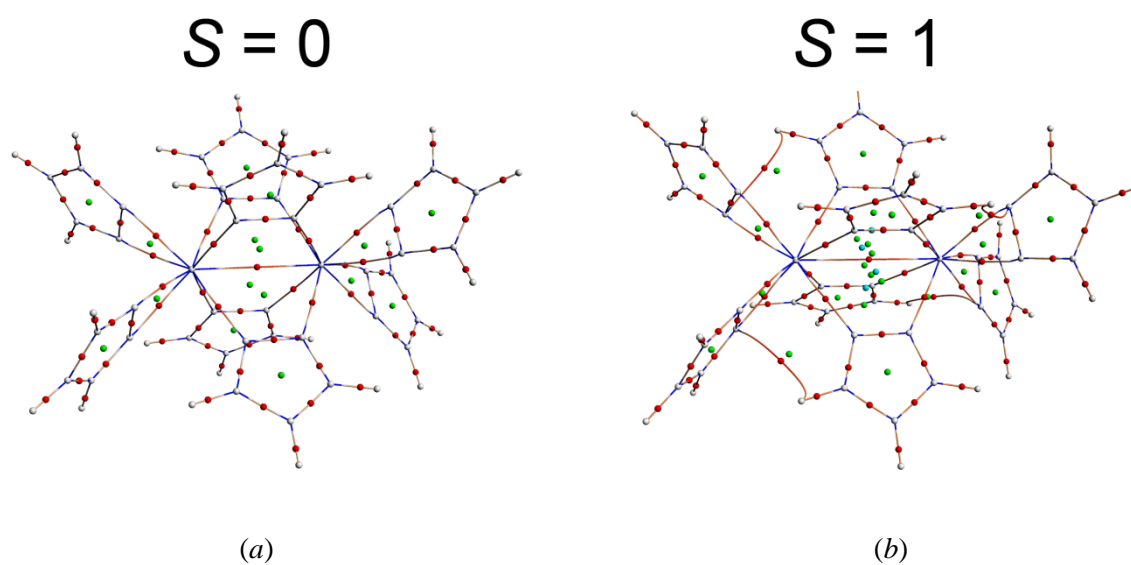


**Figure S7.** Critical points (cp's) of electronic density: (a) Singlet spin state; (b) Triplet spin state. Red – bond cp; green – ring cp, blue – cage cp, grey – atom attractors.

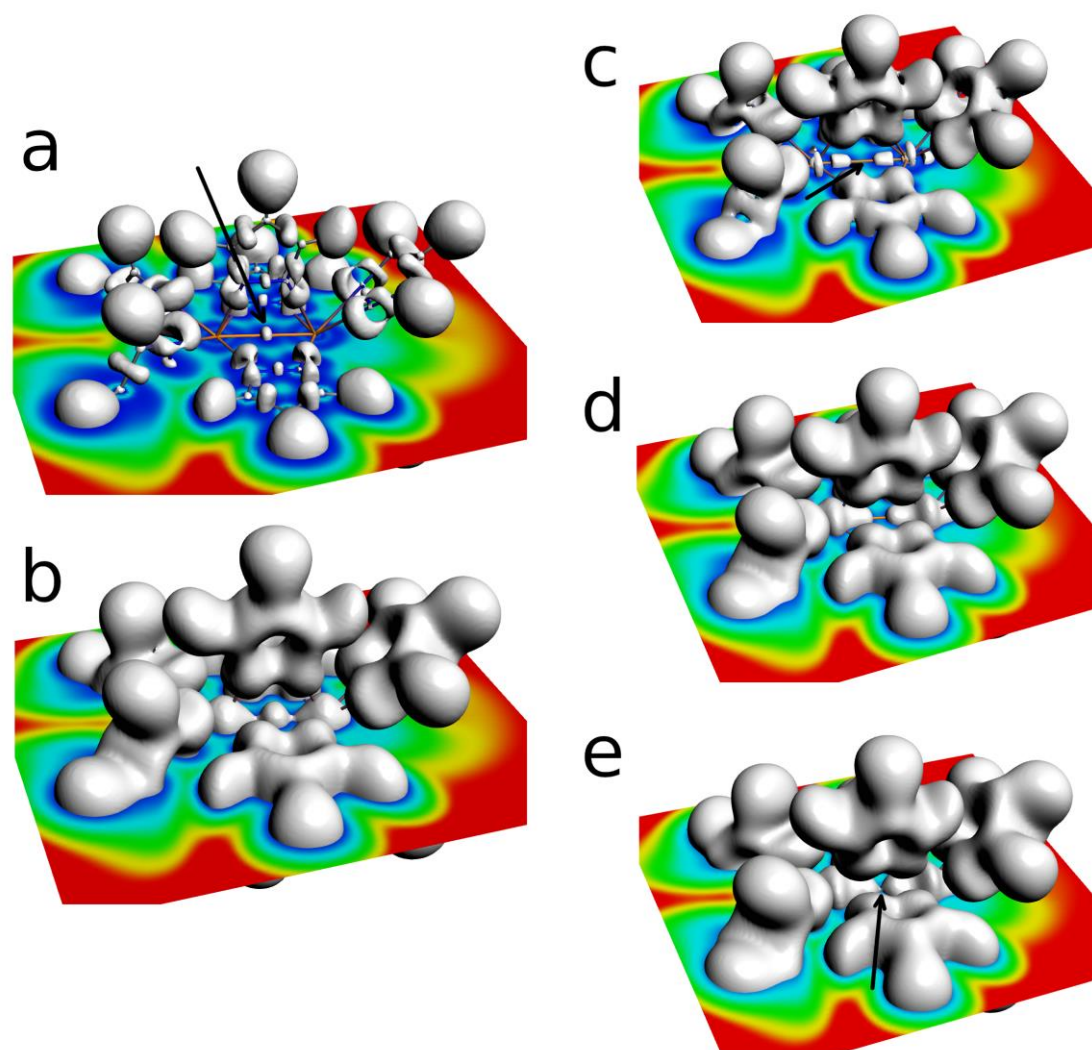


**Figure S8.** ELF cut planes and isosurfaces: singlet spin state isovalues = 0.8 (*a*) and 0,5 (*b*); triplet spin state isovalues = 0,6 (*c*), 0,4 (*d*), and 0,25 (*e*).

**Table S3.** Energy components and electron density function values in the Ta–Ta bcp\*

	Distance, Å	BP, Å	$\rho$	$\nabla^2\rho$	$G_{cp}$	$V_{cp}$	$H_{cp}$	$H_{cp}/\rho$	$ V_{cp} /G_{cp}$	$\zeta_{cp}$
$S=0$	3.145048	3.145048	0.0470	-0.0186	0.014	-0.034	-0.019	-0.407	2.321	22.681
$S=1$	3.600986	3.600986	0.0153	0.0209	0.006	-0.007	-0.001	-0.063	1.155	3.102

\* $\rho$  — electron density;  $\nabla^2\rho$  — its Laplacian;  $G_{cp}$ ,  $V_{cp}$ ,  $H_{cp}$  — kinetic (estimated using the Abramov's approximation [13]), potential and total energy densities at the bcp;  $\zeta_{cp}$  — metallicity index.

## References

---

- 1 Velde, G.t.; Bickelhaupt, F.M.; Baerends E.J.; Guerra C.F.; Gisbergen, S.J.A.v.; Snijders, J.G.; Ziegler, T. *J. Comput. Chem.* 2001, **22**, 931–967.
- 2 ADF2019, SCM, Theoretical Chemistry, Vrije Universiteit, Amsterdam, The Netherlands, <http://www.scm.com>.
- 3 Lenthe, E.v.; Baerends, E.J. *J. Comput. Chem.* 2003, **24**, 1142–1156.
- 4 Lenthe, E.v.; Ehlers, A.E.; Baerends, E.J. *J. Chem. Phys.* 1999, **110**, 8943–8953.
- 5 Vosko, S.H., Wilk, L., Nusair, M. *Can. J. Phys.* 1980, **58**, 1200–1211.
- 6 Becke, A.D. *Phys. Rev.* 1988, **A38**, 3098–3100.
- 7 Perdew, J.P. *Phys. Rev.* 1986, **B33**, 8822–8824.
- 8 Bruker AXS Inc. (2000-2012). *APEX2 (Version 2.0)*, *SAINT (Version 8.18c)*, and *SADABS (Version 2.11)*, Bruker Advanced X-ray Solutions. Madison, Wisconsin, USA.
- 9 Sheldrick, G.M. *Acta Crystallogr.* 2008, **A64**, 112–122.
- 10 Sheldrick, G.M. *Acta Crystallogr.* 2015, **C71**, 3–8.
- 11 Dolomanov, O.; Bourhis, L.J.; Gildea, R.; Howard, J.A.; Puschmann, H. *J. Appl. Crystallogr.* 2009, **42**, 339–341.
- 12 Groom, C.R.; Bruno, I.J.; Lightfoot, M.P.; Ward, S.C. *Acta Crystallogr.* 2016, **B72**, 171–179.
- 13 Abramov, Y.A. *Acta Cryst.* 1997, **A53**, 264–272.